BBA - Bioenergetics 1860 (2019) 148062

Contents lists available at ScienceDirect

BBA - Bioenergetics

journal homepage: www.elsevier.com/locate/bbabio

Discriminating changes in intracellular NADH/NAD^+ levels due to anoxicity and H_2 supply in *R. eutropha* cells using the Frex fluorescence sensor

S. Wilkening[a], F.-J. Schmitt[a], O. Lenz[a], I. Zebger[a], M. Horch[a,b], T. Friedrich[a,*]

[a] Technische Universität Berlin, Institut für Chemie PC 14, Straße des 17. Juni 135, 10623 Berlin, Germany
[b] Department of Chemistry and York Biomedical Research Institute, University of York, YO10 5DD, United Kingdom

ARTICLE INFO

Keywords:
Fluorescence sensor protein
Redox sensing
NADH
NAD^+
Frex
R. eutropha
Soluble hydrogenase
Light-driven bio-hydrogen production

ABSTRACT

The hydrogen-oxidizing "Knallgas" bacterium *Ralstonia eutropha* can thrive in aerobic and anaerobic environments and readily switches between heterotrophic and autotrophic metabolism, making it an attractive host for biotechnological applications including the sustainable H_2-driven production of hydrocarbons. The soluble hydrogenase (SH), one out of four different [NiFe]-hydrogenases in *R. eutropha*, mediates H_2 oxidation even in the presence of O_2, thus providing an ideal model system for biological hydrogen production and utilization. The SH reversibly couples H_2 oxidation with the reduction of NAD^+ to NADH, thereby enabling the sustainable regeneration of this biotechnologically important nicotinamide cofactor. Thus, understanding the interaction of the SH with the cellular NADH/NAD^+ pool is of high interest. Here, we applied the fluorescent biosensor Frex to measure changes in cytoplasmic [NADH] in *R. eutropha* cells under different gas supply conditions. The results show that Frex is well-suited to distinguish SH-mediated changes in the cytoplasmic redox status from effects of general anaerobiosis of the respiratory chain. Upon H_2 supply, the Frex reporter reveals a robust fluorescence response and allows for monitoring rapid changes in cellular [NADH]. Compared to the Peredox fluorescence reporter, Frex displays a diminished NADH affinity, which prevents the saturation of the sensor under typical bacterial [NADH] levels. Thus, Frex is a valuable reporter for on-line monitoring of the [NADH]/[NAD^+] redox state in living cells of *R. eutropha* and other proteobacteria. Based on these results, strategies for a rational optimization of fluorescent NADH sensors are discussed.

1. Introduction

Ralstonia eutropha is a gram-negative β-proteobacterium endowed with a versatile and adaptive metabolism. The bacterium is able to oxidize organic compounds, preferably organic acids (heterotrophic growth), but is also capable of exploiting CO_2 and molecular hydrogen (H_2) as carbon and energy sources (lithoautotrophic growth), respectively [1]. The ability to metabolize H_2 is mediated by four distinct [NiFe] hydrogenases in *R. eutropha* [2] that catalyze the (reversible) oxidation of molecular hydrogen in the presence of oxygen (O_2) [3]. Two of these O_2-tolerant hydrogenases are directly involved in energy conversion processes of the bacterium. The membrane-bound hydrogenase (MBH) oxidizes molecular hydrogen and channels the released electrons *via* a membrane-linked cytochrome *b* into the respiratory chain [4]. The second hydrogenase is the cytoplasmic soluble hydrogenase (SH), which couples H_2 oxidation to the reduction of oxidized nicotinamide adenine dinucleotide (NAD^+) to NADH [5]. NADH can then be used as a reducing agent for, *e.g.*, CO_2 fixation *via* the Calvin-Benson-Bassham cycle or for ATP generation *via* the respiratory chain [1]. Although biased towards H_2 oxidation, the SH is also capable of proton reduction and H_2 evolution under sufficiently reducing conditions in the cytoplasm [6]. A crucial parameter to estimate the reduction potential of the cytoplasm is the [NADH]/[NAD^+] ratio, as it (co-) defines the redox states of all the cellular NAD(H)-dependent enzymes and thus their catalytic activity [7]. Due to its high synthesis rate in living cells, both under aerobic and microaerobic conditions, the bidirectional SH activity affects the [NADH]/[NAD^+] ratio significantly. It has therefore been postulated that a spectroscopic approach, which

Abbreviations: cpFP, circularly permuted fluorescent protein; cpYFP, circularly permuted yellow fluorescent protein; FGN, fructose-glycerol-nitrogen (medium); FN, fructose-nitrogen (medium); Frex, fluorescent Rex; GN, glycerol-nitrogen (medium); LB, Lysogeny Broth (medium); MBH, membrane-bound hydrogenase; NAD, nicotinamide adenine dinucleotide; NAD^+, oxidized nicotinamide adenine dinucleotide; NADH, reduced nicotinamide adenine dinucleotide; NADP, nicotinamide adenine dinucleotide phosphate; NADPH, reduced nicotinamide adenine dinucleotide phosphate; $NADP^+$, oxidized nicotinamide adenine dinucleotide phosphate; OD, optical density; RH, regulatory hydrogenase; SH, soluble NAD^+-reducing hydrogenase; YFP, yellow fluorescent protein

* Corresponding author.
E-mail address: friedrich@chem.tu-berlin.de (T. Friedrich).

https://doi.org/10.1016/j.bbabio.2019.148062
Received 20 March 2019; Received in revised form 23 July 2019; Accepted 10 August 2019
Available online 13 August 2019
0005-2728/ © 2019 Elsevier B.V. All rights reserved.

combines the measurement of intracellular [NADH]/[NAD^+] levels with the functional state of the SH in living cells, would be highly beneficial for understanding the catalytic and physiological impact of this enzyme [8].

Many approaches have been utilized to measure the [NADH]/[NAD^+] ratio as well as the individual concentrations of both nicotinamide derivatives in living cells, each with its own advantages and drawbacks. The simplest, yet utterly challenging, approach is to utilize the inherent fluorescence of NADH to estimate cellular concentrations [9]. However, this method does not allow estimating the ratio between the reduced and oxidized forms, since NAD^+ itself is not fluorescent. Furthermore, the fluorescence of NADH occurs in a spectral region that severely overlaps with cellular autofluorescence [10]. Also, the phosphorylated congener, NADPH, mostly involved in anabolic reactions, cannot be distinguished from NADH by standard fluorescence spectroscopy. Thus, the more demanding method of fluorescence lifetime analysis is required to discriminate these molecular species [11]. However, a quantitative analysis by fluorescence lifetime imaging microscopy (FLIM) is difficult, because complex cellular samples usually show autofluorescence with multiexponential decay kinetics and ambiguous spectral shape.

Other approaches rely on lysis of cells and the investigation of [NADH]/[NAD^+]-dependent redox couples, *e.g.*, lactate and pyruvate, which are coupled to [NADH] and [NAD^+] *via* the lactate dehydrogenase reaction [12,13]. However, since cells must be disrupted, online monitoring of nicotinamide cofactor levels in living cells is impossible with this method.

Recently, genetically engineered fluorescence sensors for the monitoring of [NADH] and [NADH]/[NAD^+] in mammalian cell lines have been developed [14–17]. These sensors consist of bacterial NADH-binding proteins (so-called Rex repressor proteins) fused to a circularly permuted fluorescent protein (cpFP) [18], whose fluorescence response is highly sensitive towards structural changes. The Rex protein undergoes a significant conformational change upon NADH binding [19,20], which, in turn, modulates the fluorescence response of the cpFP.

Although derived from bacterial Rex repressor proteins, the [NADH] or [NADH]/[NAD^+] sensors developed to date (Peredox [15], Frex/FrexH [16] and SoNar [21]) have been optimized for mammalian cell lines. Importantly, the total cellular NADH/NAD^+ pools and their ratio may differ substantially in mammalian and bacterial cells [22–24]. Indeed, the Peredox sensor (designed to report the [NADH]/[NAD^+] ratio) was found to operate close to its saturation level when produced in *R. eutropha* cells grown under aerobic conditions, because its NADH sensitivity is in the lower nanomolar range [16,25]. Therefore, fluorescence sensors with diminished NADH affinity might be advantageous for their application in bacterial cells. Among the various genetically designed fluorescence probes, the Frex sensor has been constructed from the *Bacillus subtilis* Rex protein (genetically optimized to have a lower NADH sensitivity) and the circularly permuted yellow fluorescent protein, cpYFP [16], serving as the chromophore. This sensor was initially established as a tool for determining absolute [NADH].

The goal of this work is to use the Frex sensor for sensing relative changes in NADH levels in *R. eutropha*, taking advantage of its lower NADH sensitivity compared to Peredox [25], but still bearing in mind the complex interaction of Frex with NADH and NAD^+ based on our previous work [26]. At NAD^+ concentrations exceeding 100 µM, the oxidized nicotinamide cofactor competes markedly with NADH for the binding site [27] and, thereby, reduces the maximal fluorescence response of the Frex sensor in a concentration-dependent manner [26]. However, since the cellular [NAD^+] is about two orders of magnitude larger than [NADH] [22,23], even large relative changes in [NADH] would typically be translated into small absolute changes in [NAD^+]. Consequently, any variation of the Frex fluorescence amplitude should predominantly report just [NADH] changes, while the corresponding [NAD^+] variations affect the sensor response only moderately. Indeed, our data show that upon Frex synthesis in *R. eutropha*, its fluorescence signal dynamically reflects changes of cellular [NADH] during the shift from aerobic to anaerobic conditions and in response to the availability of H_2, which can be unequivocally assigned to the activity of the SH.

2. Materials and methods

2.1. Cloning of Frex gene into the pLO13-SH vector

The cDNAs coding for Frex and cpYFP (kind gift from Dr. William Oldham and Prof. Joseph Loscalzo, Harvard Medical School) were cloned into the pLO13-SH vector between the restriction sites of *Nco*I and *Hind*III. The *Nco*I restriction site was introduced by site-directed mutagenesis via recombinant PCR. PCR amplification primers were:

Forward Primer Frex: 5′-CGATAAGGAGCCCATGGATAAGG-3′
Forward Primer cpYFP: 5′-GGCTACCATGGCGGATCCG-3′
Reverse Primer: 5′-GCTAGTTATTGCTCAGCGG-3′

The pLO13-SH vector carries a tetracycline resistance gene, and transcription of the subcloned cDNA is under the control of the endogenous promoter for the soluble hydrogenase (SH).

2.2. Conjugation of Frex- and cpYFP-pLO13-SH plasmids into the desired R. eutropha strains

E. coli S17-1 cells were transformed with the pLO13-SH plasmid vectors carrying the cDNA of the fluorescent (sensor) protein and grown overnight in 10 mL of LB medium containing 10 µg/mL tetracycline. Recipient *R. eutropha* strains HF798 (SH^+, MBH^-, regulatory hydrogenase$^-$ (RH^-)) and HF500 (SH^-, MBH^-, RH^-) [28,29] were also cultivated overnight in 10 mL LB medium. Cells were harvested and washed with 5 mL of sterile H16 buffer (24 mM $Na_2HPO_4{\cdot}7H_2O$, 11 mM KH_2PO_4) and resuspended in 1 mL of sterile H16 buffer. 200 µL of donor and recipient strains were given onto a LB agar plate and mixed by spot mating. After 6 h of incubation at 37 °C, the cells were scraped off the plate with a sterile glass pipette, washed in 5 mL of sterile H16 buffer, and resuspended in 1 mL of sterile H16 buffer. 100 µL of 10^{-4}-fold diluted samples were streaked onto an FN (composition see below) agar plate containing 10 µg/mL tetracycline and grown for 3 days at 37 °C. Transconjugant colonies appeared, and incorporation of the desired plasmid was checked by alkaline lysis (pH 12) of cells expressing Frex.

2.3. Growth of R. eutropha

R. eutropha cells were grown in FN medium (24 mM $Na_2HPO_4{\cdot}7H_2O$, 11 mM KH_2PO_4, 37 mM NH_4Cl, 0.81 mM $MgSO_4{\cdot}7H_2O$, 68 µM $CaCl_2{\cdot}2H_2O$, 11 µM $FeCl_3{\cdot}6H_2O$, 1 µM $NiCl_2$, 0.4% fructose, pH 7.3) or FGN medium (FN medium with 0.2% fructose and 0.2% glycerol) at 30 °C. Cells were grown to an OD_{600} of 7 in the presence of 10 µg/mL tetracycline. Before fluorescence measurements of cells, tetracycline had to be removed from the medium, since the emission spectra of tetracycline and the Frex sensor overlap. Thus, cells were harvested and resuspended to a final OD_{600} of 0.5 in fresh tetracycline-free GN medium (24 mM $Na_2HPO_4{\cdot}7H_2O$, 11 mM KH_2PO_4, 37 mM NH_4Cl, 0.81 mM $MgSO_4{\cdot}7H_2O$, 68 µM $CaCl_2{\cdot}2H_2O$, 11 µM $FeCl_3{\cdot}6H_2O$, 1 µM $NiCl_2$, 0.4% glycerol, pH 7.3).

2.4. Alkaline lysis

R. eutropha cells were grown heterotrophically, harvested, and resuspended to a final OD_{600} of 0.5 in H16 buffer (24 mM $Na_2HPO_4{\cdot}7H_2O$, 11 mM KH_2PO_4) at pH 11. Cells were incubated for 15 min, leading to lysis of the cells due to the alkaline environment. Suspensions of disrupted cells were subsequently examined by fluorescence spectroscopy.

2.5. Gas incubation

1 mL aliquots of cell suspensions with a final OD_{600} of 0.5 were bubbled for various time periods in a 2 mL quartz cuvette sealed with a rubber septum at a gas flow rate of 0.1 L/min at room temperature. Spectra were recorded immediately afterwards.

2.6. Gas mixtures

Cell suspensions with a final OD_{600} of 0.5 were added to a mixture of aerated GN medium and H_2-saturated GN medium in appropriate volume combinations to obtain the desired H_2 percentages. Cuvettes for fluorescence measurements were completely filled by the fluid phase.

2.7. Fluorescence measurements

Fluorescence was measured with a Fluoromax-2 spectro-fluorometer (Horiba Jobin Yvon, Bensheim, Germany). Slits were set to 4 nm for excitation and 2 nm for emission, while the integration time was 1 s and the increment 1 nm. Frex was excited at 480 nm, and emission spectra were recorded in a suitable range centred around the emission maximum of 515 nm for evaluation of the amplitudes. cpYFP was excited at 480 nm for comparability of the fluorescence response with the derived sensors.

The titration data of the acquired fluorescence intensity F of Frex in lysed cells were analyzed by means of the Hill equation,

$$F = \frac{F_{max} \cdot [NADH]^n}{K_D^n + [NADH]^n} \quad (1)$$

in which F_{max} is the fluorescence in the presence of fluorescence-saturating NADH concentrations, K_D is the microscopic dissociation constant, and n is the cooperativity parameter.

Another approach to determine the dissociation constant K_D for the situation in lysed cells uses a quadratic formula to fit the titration data. In contrast to a classical hyperbolic curve (such as the Hill function in Eq. (1)), the underlying model is free from assumptions regarding the concentrations of total and free titrant (receptor) and the binding stoichiometry [30,31].

$$\frac{[RL]}{[R_{tot}]} = \frac{[L_{tot}] + [R_{tot}] + K_D}{2.\,[R_{tot}]} - \sqrt{\left(\frac{[L_{tot}] + [R_{tot}] + K_D}{2.\,[R_{tot}]}\right)^2 - \frac{[L_{tot}]}{[R_{tot}]}} \quad (2)$$

In this formula, $[RL]$ is the concentration of the Frex sensor protein with NADH bound (here reflected by the normalized fluorescence amplitude), $[R_{tot}]$ is the total concentration of equivalent receptor binding sites (in μM), $[L_{tot}]$ is the total concentration of NADH present ("ligand"), and K_D represents the dissociation constant. Fitting the data using this equation yields two fit parameters, $[R_{tot}]$ and K_D. If the binding stoichiometry n is known, the total receptor concentration can be calculated from the ratio $[R_{tot}]/n$.

Data processing was carried out using Origin 2017 software (OriginLab Corp., Northampton, MA, U.S.A.).

3. Results

The cDNA for the Frex sensor was subcloned into the pLO13-SH vector, as described in Materials and Methods and previously [25]. The resulting plasmid was introduced into the SH-expressing and SH-deficient *R. eutropha* strains HF798 (SH^+, MBH^-, RH^-) and HF500 (SH^-, MBH^-, RH^-), respectively [28,29]. Since the fluorescence of the cpYFP moiety of the sensor increases strongly at alkaline pH [32], expression and functionality of the Frex sensor was confirmed *via* alkaline lysis of cells and subsequent measurement of the Frex fluorescence signal upon this alkaline treatment (Supplementary Fig. 1).

We first aimed at inferring changes in cytoplasmic [NADH] by monitoring the fluorescence of Frex to establish a relationship between Frex fluorescence and SH activity by comparing Frex fluorescence in SH-synthesizing and SH-deficient *R. eutropha* strains. Therefore, we sought to elevate Frex fluorescence by treating Frex-synthesizing cells with H_2. To delimit the effect of the H_2-driven NAD^+ reduction activity of the SH on the cellular NADH pool from the more general effects of anoxic conditions and concomitant overreduction of the cytoplasm, we carried out control experiments with helium (He) treatment.

In a first set of experiments, Frex-containing *R. eutropha* cultures were treated with H_2 gas in a septum-sealed quartz cuvette under constant stirring, until a steady-state fluorescence amplitude was reached (10 min). This treatment led to a strong increase in the Frex fluorescence signal by about the same factor for the cells of both *R. eutropha* HF798 and HF500 (Fig. 1A,B).

The robust increase of the Frex signal upon H_2 treatment (Fig. 1A,B) indicates an increase in cytosolic [NADH]. This is in line with the expectation that treatment of *R. eutropha* cells with H_2 removed all O_2 from the samples. Since O_2 serves as the terminal electron acceptor of the respiratory chain [1], its absence prevents NADH from being re-oxidized by respiratory complex I (NADH:ubiquinone oxidoreductase), and NADH should accumulate in the cytoplasm. Notably, upon H_2 treatment, the fluorescence of the Frex sensor increases more than eightfold in both strains (Fig. 1A,B) indicating that the removal of O_2 and the concomitant blockage of the respiratory chain is mainly responsible for the acute rise in [NADH], irrespective of the presence or absence of the SH. Based on our previous study on the purified Frex protein, an eightfold increase of the Frex fluorescence corresponds to the maximal extent of sensor signal augmentation at neutral pH. This dynamic range can only be achieved if the sensor response is saturated by NADH, and the free NAD^+ concentration in the cells is below 100 μM; otherwise NAD^+ would limit the maximal Frex response to NADH, as shown previously [26].

To test the hypothesis that O_2 removal is the main factor determining the acutely elevated [NADH] levels independent from the presence of SH, anoxic conditions were also induced by treatment with He gas (Fig. 1A,B). Upon He treatment, an elevated Frex signal of comparable relative amplitude was again observed in both (SH-expressing and SH-deficient) strains, and a rather fast signal decrease to the initial level occurred upon re-aeration (Fig. 1D,F) similar to the time course of the Frex signal observed for SH-deficient HF500 cells upon H_2-treatment (Fig. 1E). The Frex signal increase caused by He treatment reached only 50% of that of H_2-treated cells. This behaviour might demand further elucidation, but since the same result was obtained for both *R. eutropha* strains (Fig. 1A,B), it is obviously not related to the presence or absence of SH activity. The observed differences might rather hint at the influence of the different physico-chemical properties of the two gases on the complex cellular response that eventually governs the $NADH/NAD^+$ levels in an anoxic response. For example, different Henry constants [33], diffusion constants [34] or water/lipid partition coefficients would all influence the availability of a particular gas in cells.

Remarkably, we found no significant difference regarding the H_2-mediated *relative* increase of Frex fluorescence intensity in both strains (note that the overall fluorescence amplitudes in these experiments is dependent on cell density and expression level of the sensor). Thus, the immediate increase of the sensor fluorescence alone does not allow for discriminating effects on cellular [NADH] related to the presence of SH. However, the time courses of the decline of the fluorescence signals during re-aeration of the H_2-exposed cells were strikingly different for

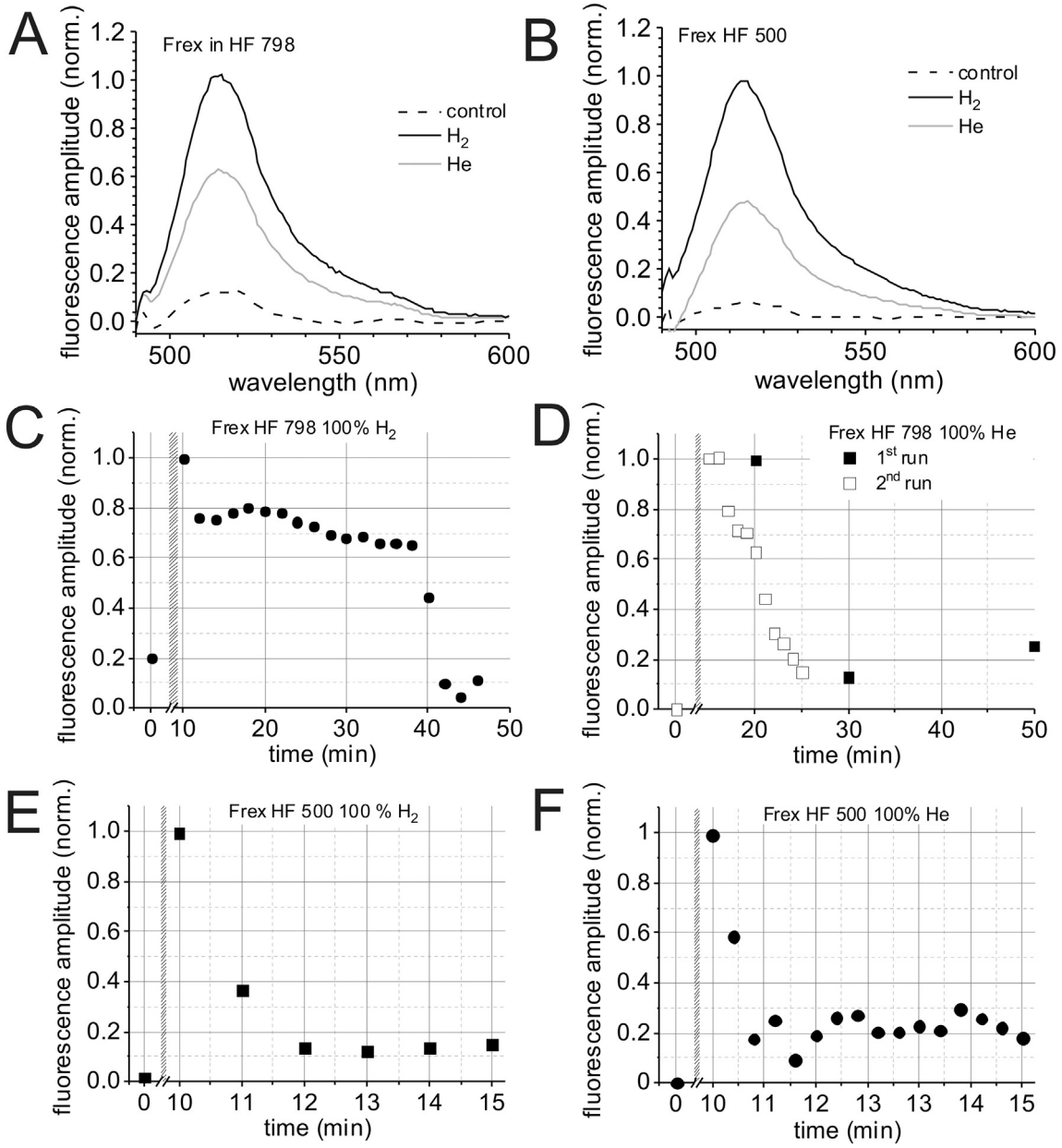

Fig. 1. (A,B) Background-corrected and normalized fluorescence spectra of Frex-containing *R. eutropha* cell suspensions of the same OD_{600} after excitation at 480 nm (see Supplementary Fig. 2 for the background subtraction procedure). The relative increase in Frex fluorescence is higher for H_2 treatment than for helium treatment in both, the SH-expressing strain HF798 (A) and the SH-deficient strain HF500 (B), indicating that these immediate responses to anoxic conditions occur independent from the presence or absence of the SH. (C,D) Frex fluorescence response in the SH-expressing strain HF798 during and after treatment with H_2 (C) and helium (D). Panel (D) summarizes two experiments conducted on different time scales. (E,F) Frex fluorescence response in the SH-deficient strain HF500 during and after treatment with H_2 (E) and helium (F). Samples in (C) to (F)—were treated in a sealed fluorescence cuvette with H_2/He gas until the signal was stable, and then the septum was removed (axis break). Data points in (C) to (F)—refer to background-corrected fluorescence levels at 515 nm (excited at 480 nm) normalized to values between 0 and 1, with 0 being the lowest fluorescence amplitude (at the Frex emission peak around 515 nm) and 1 the corresponding maximum amplitude measured immediately after removal of the septum.

the two strains. In SH-deficient cells (HF500), the signal decreased to the initial basal value after about 2 min of aeration (Fig. 1E). In contrast, for the SH-expressing cells of the HF798 strain, the signal stayed elevated for about 30 min after re-exposure to atmospheric O_2, and only after this period, the signal dropped sharply over the course of about 1 min to the initial value (Fig. 1C). This indicates that in the presence of H_2, continuous activity of SH leads to a steadily elevated [NADH] in strain HF798 (as long as H_2 is available, see below) but not in the SH-deficient strain HF500.

At present, it is impossible to derive reliable quantitative information about NADH/NAD^+ concentrations from the observed sensor responses, since the interaction of NADH and NAD^+ with the Frex sensor is complex, as exemplified by the fact that the dynamic range of the sensor is limited, if NAD^+ concentrations exceed 100 μM [26]. Thus, without further knowledge about the actual NAD(H) pool size, it is impossible to discriminate, whether the 50-%-reduced response of the sensor in He- versus H_2-treated cells is, for example, due to a half-maximal NADH concentration (3.5 μM) at zero [NAD^+] or due to the presence of 100 μM NADH at about 400 μM NAD^+ (see Figs. 1 and 2 in [26]). However, the very similar temporal Frex response pattern observed upon He treatment and subsequent re-aeration (Fig. 1D,F) shows that under anoxic conditions and recovery thereof, the cellular response

is apparently independent from the presence of the SH. Upon limitation of the terminal electron acceptor O_2, NADH accumulates, but, as soon as O_2 is available again, the fluorescence signal decreases on a relatively short time scale due to respiratory NADH consumption. In contrast, the constant high-level signal of the sensor, which only occurred in SH-expressing cells after H_2 treatment (Fig. 1C) indicates sustained elevation of [NADH] due to the activity of the SH. The enzyme should be able to produce NADH as long as sufficient H_2 concentrations are present in the cells during the recovery of atmospheric conditions (see below). This indicates that under the chosen experimental conditions, sufficient H_2 is available for a certain time span (during re-exposure to air), before it is depleted from the solution by diffusion or consumption by the SH.

A caveat for using the Frex sensor in living cells is its pronounced pH-sensitivity, which is inherited from the cpYFP fluorophore [16,32,35]. cpYFP fluorescence can also be used to monitor possible intracellular pH changes. To delineate, whether cytoplasmic pH changes occur during the chosen experimental conditions, gas exchange experiments were carried out with *R. eutropha* cells synthesizing just the cpYFP fluorophore. When cpYFP-containing *R. eutropha* cells, cultivated under the same conditions as the Frex expressing cells used for the experiments shown in Fig. 1, were subjected to the same H_2 treatment as described in Fig. 1 or to anaerobic conditions by flushing with He gas, the fluorescence amplitude did not change significantly (Supplementary Fig. 3). Thus, substantial pH changes influencing the sensor's response can be excluded. Since the cpYFP fluorescence signal of intact cells was rather small, we needed to ascertain appropriate expression of cpYFP. For this purpose, the cells used for the experiments shown in Supplementary Fig. 3 were subsequently lysed by resuspension in pH 11 buffer. After this treatment, strongly elevated fluorescence signals were observed, which demonstrates robust cpYFP synthesis in both *R. eutropha* strains. These control experiments support the notion that the Frex signals observed under the conditions in living cells are not biased by concomitant pH changes in the cytoplasm.

Another set of experiments aimed at a differentiated response of the Frex sensor to different H_2/O_2 ratios. For this purpose, pelleted cells were resuspended in different mixtures of a buffer equilibrated with the oxic atmosphere and another buffer saturated with H_2. By mixing these two buffers in different ratios and filling the cuvette completely, different H_2 partial pressures could be realized while still having substantial O_2 in the samples. These experiments revealed that the more H_2 is available as SH substrate, which is metabolized to produce NADH, the longer the Frex fluorescence signal remains at an elevated level (Fig. 2A). The duration of elevated fluorescence shows a monotonous increase with increasing H_2 partial pressure, whereas the maximal increase in fluorescence did not depend on this parameter (Fig. 2A). This supports the finding of Fig. 1C that the Frex fluorescence signal stays elevated until all H_2 is consumed by SH (or diffused into the atmosphere) so that the NADH level drops significantly below the saturation level of the sensor.

This indicates that even the lowest H_2 concentration applied (10% of partial pressure corresponds to about 80 μM H_2 as inferred from the Henry constant of H_2 in aqueous solution, see [33]) was sufficient to allow the SH to produce [NADH] exceeding the saturation limit of the Frex sensor. Therefore, rather than the fluorescence intensity, which might be saturated over a wide range of H_2 concentrations, the time duration of the elevated sensor fluorescence serves as a marker for the activity of the SH in living cells (Fig. 2B) in relation to availability of H_2.

Since the H_2 concentration in the cell suspensions directly relates to the duration of elevated fluorescence, it should also be possible to alter the duration of elevated fluorescence not by changing substrate (H_2) concentration but by changing the amount of cells (i.e. the cell density) able to consume a given H_2 concentration. This was verified by exposing HF798 cell suspensions of different optical densities to the same H_2 partial pressure (Fig. 3).

To correlate the observed times of elevated (saturated) Frex sensor fluorescence in experiments on *R. eutropha* cell suspensions in buffers with different H_2 partial pressures (Fig. 2) or with different cell densities (OD_{600} values, Fig. 3) with the activity of the SH, we performed a hydrogenase activity assay. For this, *R. eutropha* cell suspensions were diluted to a certain OD in an H_2-saturated buffer containing 1 mM NAD^+ and 0.005% (w/v) of the surfactant cetyltrimethylammonium bromide (CTAB) to permeabilize the cells (see Supplementary Information). The metabolic activity of the hydrogenase was monitored by the increase of the NADH absorbance (extinction coefficient) at 365 nm over time. From these experiments, the NADH-producing activity of a cell lysate obtained from a suspension of cells of a certain OD could be determined. The H_2 concentration of a 100% H_2-saturated aqueous solution is about 800 μM, as calculated from the corresponding Henry constant of H_2 gas [33], and H_2 concentrations at lower percentages can be determined, accordingly. With these [H_2] values and the metabolic activity stated above, one can calculate the "reaction times" (t_{calc}), which *R. eutropha* cell suspensions of a given OD would need to metabolize a given [H_2], in order to compare these with the experimentally observed times (t_{exp}) of elevated Frex fluorescence from Figs. 2B and 3, as listed in Supplementary Tables 1 and 2. Of note, the calculated "reaction times" were in good agreement with the

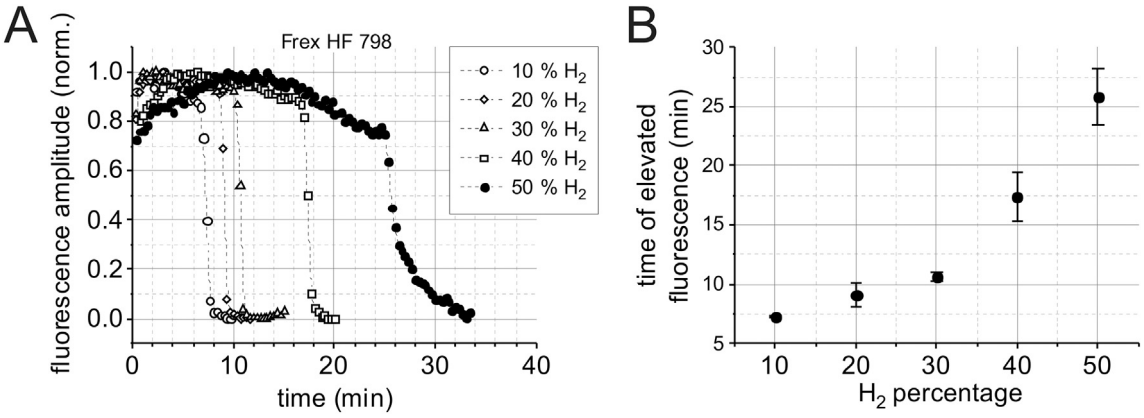

Fig. 2. (A) Frex fluorescence in the presence of specified H_2/air mixtures (H_2 content in % v/v as indicated) in the SH-expressing strain HF798. Excitation was carried out at 480 nm, and fluorescence emission maxima at 515 nm were plotted at various time points. Fluorescence signals were background-corrected and subsequently normalized to values between 0 and 1, with 0 being the lowest fluorescence amplitude (at the Frex emission peak around 515 nm) and 1 the corresponding maximum amplitude measured in the experiment. (B) Influence of the applied H_2 percentage in the gas mixture (partial pressure) on the duration of elevated Frex fluorescence (time for signal decrease to 50% of the saturation value from experiments in panel (A)).

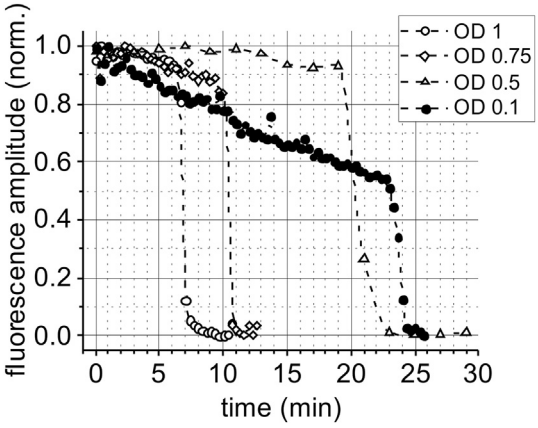

Fig. 3. Frex fluorescence signals in the presence of 50% H_2 in *R. eutropha* HF798 cell suspensions of differing OD. Frex was excited at 480 nm and the fluorescence emission maxima at 515 nm were plotted at various times. The higher the total amount of SH in the samples (due to different cell densities indicated by the OD values), the faster the substrate H_2 is metabolized. Fluorescence signals were background-corrected and subsequently normalized to values between 0 and 1, with 0 being the lowest fluorescence amplitude (at the Frex emission peak around 515 nm) and 1 the corresponding maximum amplitude measured in the experiment immediately after preparation of the samples.

experimentally determined data, the only significant deviation occurred for the experiment with low cell density (OD_{600} = 0.1).

To reveal information about the intracellular concentrations of NADH and NAD^+ in *R. eutropha*, we used a calibration technique as described previously for the fluorescence reporter Peredox in lysed cells [25]. First, the Frex-expressing cells were sonicated, which led to a strong decrease of the fluorescence signal because of the dilution of the cellular constituents upon lysis. These lysates were subsequently used for NADH and NAD^+ titration experiments while the corresponding fluorescence emission spectra were recorded (Fig. 4).

Fig. 4A shows the raw spectra obtained from the crude cell extract incubated with different amounts of NADH. The Frex sensor retained functionality after lysis and shows a dose-dependent response towards NADH. Compared to previous experiments on the purified sensor protein [26], in which an increase of the Frex fluorescence signal was already observed at 1 μM NADH, somewhat higher NADH concentrations ([NADH] ≥ 5 μM) were required to enhance the sensor emission above the background signal. At [NADH] higher than 500 μM, the fluorescence emission signal was saturated.

The concomitant NAD^+ titration of the crude cell extract is shown in Fig. 4B. First, a constant amount 1 mM NADH was provided to robustly induce sensor emission. Subsequently, increasing NAD^+ concentrations were added. This strategy was chosen because it has been previously shown that NAD^+ reduces the emission of the Frex sensor by competing with NADH for the binding site(s) [26]. Accordingly, we observed decreasing fluorescence signals with increasing [NAD^+]. As already mentioned for the NADH titration experiment, also for the NAD^+ titration a somewhat larger concentration was needed to induce a significant signal decrease compared to the value determined with purified protein [26]. Such deviations, which result in larger apparent K_D values determined from curve fitting, could arise if the concentration of the Frex sensor in the cell lysates would be in the same range as the K_D determined under well-defined conditions on the purified Frex protein [30,31]. It also seems likely that the debris of cell constituents or membranes non-specifically scavenges NAD(H) to reduce the free NAD(H) concentration.

For quantitative data analysis, the spectra were background-corrected by subtracting the first spectrum after lysis (recorded at zero [NADH] or [NAD^+]) from the subsequently recorded titration spectra. The spectra recorded in the absence of exogenously added nicotinamide cofactors do not show a significant contribution of Frex-specific emission and resemble the scattering background of the turbid lysates. Peak intensities of the background-corrected spectra at 515 nm were then normalized to values between 0 and 1, plotted against the NADH concentration (Fig. 4C), and fitted by a Hill function (Eq. (1)) with the parameters shown in the inset. The calculated K_D value (microscopic dissociation constant) was (19.6 ± 1.7) μM (with a Hill coefficient 1.7 ± 0.2), which is larger than the K_D value of 3.5 μM determined previously for the purified Frex protein [26]. For a better analysis, we used a quadratic formula (Eq. (2)) for fitting the data, which is derived from a reaction model that is free from assumptions regarding the concentrations of total and free titrant (receptor) as well as the binding stoichiometry [30,31]. This model function compensates for the unknown receptor/sensor concentration, while determining the real dissociation constant. The K_D value derived from this fit (Fig. 4D) is about (5.7 ± 1.5) μM, which is in better agreement with the determined K_D from measurements using the purified sensor protein (K_D = 3.5 μM, [26]).

4. Discussion

In order to determine differences in cytoplasmic NADH levels related to the activity of the soluble hydrogenase (SH), the fluorescence sensor Frex was stably expressed in different *R. eutropha* strains either containing (strain HF798) or devoid of the SH (strain HF500). The monitoring of dynamic changes in [NADH] is of paramount importance to infer the metabolic status (redox state) of the cells. In theory, the different NADH levels in both cell strains should be attributable to the presence or absence of SH activity, especially if H_2 as substrate for the SH is available. However, control experiments are required to distinguish changes in [NADH] which are related to the activity of the SH from general effects of anaerobic conditions on the respiratory chain.

In measurements with H_2-saturated cell suspensions of strain HF798 (SH^+), a strong elevation of Frex sensor fluorescence was observed that reached a constant maximum level, which stayed constant for substantial time periods after re-aeration of the cell suspensions, and then dropped sharply to its basal value (Fig. 1C). In comparison, cells devoid of the SH showed a different time pattern of Frex sensor fluorescence. After a short fluorescence emission peak, the signal decreased upon re-oxygenation of the samples rather rapidly within about 5 min or less (Fig. 1E), a pattern that was also observed in both strains, if He treatment was used to induce anoxic conditions. Altogether, this indicates that the expressed SH in strain HF798 metabolized the supplied H_2 to yield NADH as long as sufficient H_2 is available in the system [36]. This activity of the SH keeps the [NADH]/[NAD^+] ratio sufficiently high thereby stimulating Frex fluorescence over a prolonged period of time. Therefore, the Frex sensor is a convenient tool to monitor SH activity in living cells. Remarkably, initial elevation of the Frex fluorescence signal is apparently independent from the applied H_2 partial pressure, while the duration of the elevated fluorescence under re-aeration is correlated with the previously applied H_2 partial pressure (Fig. 2A) or the cell density (Fig. 3). These findings indicate (i) that the response of the Frex sensor is rapidly driven into saturation during gas treatment due to SH-dependent NADH production – even at low H_2 partial pressures – and (ii) that the duration of the elevated fluorescence signal is indicative of the amount of SH and its substrate (H_2) present during the experiment (Figs. 2B and 3).

Thus, using the strategies established herein, the Frex [NADH] sensor is capable of determining SH activity in living cells in a variety of settings, since it shows a robust fluorescence response with a large dynamic range, which is dependent on the cellular NADH level. In contrast, the similar Peredox reporter protein with its NADH affinity in the low nanomolar range and its limited dynamic range [15,16], showed only minute fluorescence increases under the same experimental conditions [25]. Therefore, the about 100-fold lower NADH

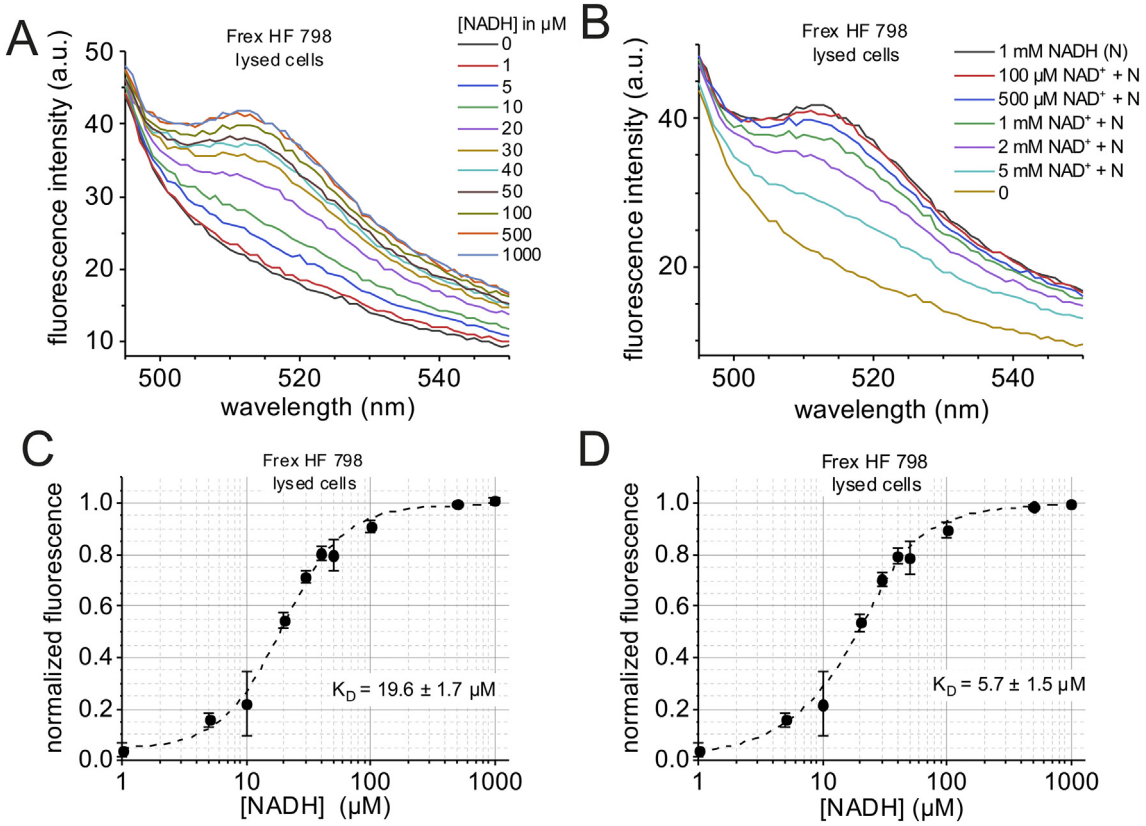

Fig. 4. Calibration for the Frex sensor response to NADH and NAD^+ in lysates of Frex-expressing cells with an OD of 0.1. (A,B) Unprocessed fluorescence emission spectra recorded in *R. eutropha* HF798 cell lysates upon excitation of Frex with 480 nm in the presence of various NADH concentrations (A) or different NAD^+ concentrations at a fixed [NADH] of 1 mM (B). Fluorescence signals were background-corrected and subsequently normalized to values between 0 and 1, with 0 being the lowest fluorescence amplitude (at the Frex emission peak around 515 nm) and 1 the corresponding maximum amplitude measured in the experiment. (C) Fits of the background-corrected and normalized fluorescence amplitudes from experiments as described in (A) with a Hill function. The resulting fit parameters are given in the inset (data from three experiments). (D) Fit of the data from (C) with a quadratic formula (Eq. (2)). The inset shows the resulting fit parameters (data from three experiments).

affinity of Frex provides a more valuable tool for NADH detection in cellular settings under which NADH concentrations in the range of up to hundreds of micromolar are common, as in bacteria, with *R. eutropha* as a biotechnologically relevant example. However, the NADH levels in *R. eutropha* cells, especially under conditions of high SH activity, apparently also exceed the K_D value of the Frex sensor by far, so that the sensor cannot report the full range of cellular NADH concentrations. To adapt to this, further tailoring of the NADH affinity of the Frex sensor would be required. Nonetheless, although the Frex fluorescence response does not differ largely in intensity when exposed to different H_2 partial pressures, it reports variant NADH levels in terms of the time period of the elevated fluorescence signal.

Even though the qualitative response of Frex can be unequivocally assigned to SH activity, it is not possible to quantitatively determine cellular NADH levels due to the antipodal effects of [NADH] and [NAD^+] on the sensor response [26]. While it was initially reported that the Frex sensor does not interact or alter fluorescence upon binding of the oxidized congener NAD^+ up to concentrations of 100 µM [16,23], we found later that NAD^+ concentrations surpassing this value reduce the NADH-dependent fluorescence signal of Frex [26], in line with the NADH/NAD^+ dependence of the parental Rex protein reported previously [27,37,38]. In living *Ralstonia eturopha* cells, Frex shows its full dynamic range (determined for the purified sensor protein upon excitation at 480 nm [26]) under conditions of sufficient H_2 supply. This indicates that the NAD^+ concentration is lowered to below 100 µM by the activity of the SH, since larger NAD^+ concentrations would limit the dynamic range of the sensor [26]. In our previous work, we estimated that the intracellular NAD^+ concentration in *R. eutropha* under aerobic conditions corresponds to 1.9 mM [25]. On the one hand, one could infer from this that the maximal Frex fluorescence under aerobic conditions in *R. eutropha* must be affected by the basal NAD^+ levels and that quantitative NADH determination is not straightforward [22,24,25]. On the other hand, the fact that H_2 treatment (and anoxic conditions) induce(s) the maximum dynamic response of the sensor, at least indicates that the activity of the SH diminishes the free intracellular [NAD^+] to (less than) 100 µM with a concomitant increase in free [NADH] into the hundreds of µM range.

A drawback to the application of Frex in living cells is that only relative changes of its fluorescence amplitudes can be evaluated, while the dynamic range is influenced by several factors including [NAD^+]. While our data show that Frex can be utilized to measure intracellular [NADH] changes in bacterial cells grown to the stationary phase, it would be of major interest to monitor the NADH/NAD^+ redox state during the exponential growth phase. However, in a growing culture, the amount of Frex sensor per volume of cell suspension increases in a complicated manner dependent on cell density, and, concomitantly, the fluorescence signal increases in such a way that a correlation with the cellular [NADH] level is impossible. To resolve this, a signal normalization procedure would be necessary to allow for calibrating to the total amount of sensor protein in the sample, e.g. by utilization of an appropriate fluorescence standard, as in the Peredox sensor [15], which carries an additional red-emitting fluorophore for this purpose. In Frex, such an intrinsic normalization procedure would theoretically be possible by utilizing excitation within the other excitation band of the cpYFP chromophore (420 nm). However, the implementation of such a concept entails other experimental difficulties, since the fluorescence

signal at 420 nm is much weaker and strongly overlaps with the cellular autofluorescence [16]. Thus, to avoid ambiguities due to the variable expression level of the sensor in cells, signal normalization could be facilitated by fusing a red fluorescent protein to Frex. Another point for improvement of the signal intensity would be to exchange the rather poor cpYFP fluorophore by a different one with a higher inherent brightness. Moreover, genetic engineering could be applied to develop sensor variants with further reduced [NADH] sensitivity, with eliminated NAD^+ sensitivity, or with sensitivity to the [NADH]/[NAD^+] ratio.

Even though the Frex sensor has inherited a profound pH-sensitivity from its precursor cpYFP [16,32,35], it could be ruled out that the sensor's response to H_2 treatment of strain HF798 was significantly influenced by concomitant pH changes in the cytoplasm (Fig. 4). In line with previous observations for mammalian cells [16], this observation indicates that cellular pH regulation in bacteria is under tight control even if large changes in the availability of metabolites are induced.

Despite certain limitations in quantitative studies, the robustness of the fluorescence signal makes the Frex sensor a promising candidate for biotechnological applications to monitor, optimize, or adjust bacterial culture conditions. Preliminary work on this approach is currently in progress and will be the subject of forthcoming studies. Future research might also utilize Frex to monitor SH activity and to correlate this information with insights from established spectroscopic approaches such as IR or EPR spectroscopy in order to gather comprehensive information in living cells regarding the active states of NAD(H)-coupled hydrogenases, their reaction mechanism, and the parameters controlling their activity.

Transparency document

The Transparency document associated with this article can be found, in online version.

Acknowledgements

The authors are grateful to Dr. William Oldham and Prof. Joseph Loscalzo (Harvard Medical School, USA) for providing the Frex expression clone. Work was funded by the Deutsche Forschungsgemeinschaft (DFG, German Research Foundation) under Germany's Excellence initiative 2005–2018 – EXC 314/1 (UniCat) and Germany's Excellence Strategy – EXC 2008/1 (UniSysCat) – 390540038.

Appendix A. Supplementary data

Supplementary data to this article can be found online at https://doi.org/10.1016/j.bbabio.2019.148062.

References

[1] R. Cramm, Genomic view of energy metabolism in *Ralstonia eutropha* H16, J. Mol. Microbiol. Biotechnol. 16 (1–2) (2009) 38–52, https://doi.org/10.1159/000142893.
[2] C. Schäfer, B. Friedrich, O. Lenz, Novel, oxygen-insensitive group 5 [NiFe]-hydrogenase in *Ralstonia eutropha*, Appl. Environ. Microbiol. 79 (17) (2013) 5137–5145, https://doi.org/10.1128/AEM.01576-13.
[3] O. Lenz, L. Lauterbach, S. Frielingsdorf, B. Friedrich, Oxygen-tolerant Hydrogenases and Their Biotechnological Potential, in: M. Rögner, De Gruyter (Eds.), Biohydrogen, 2015, pp. 61–96, , https://doi.org/10.1515/9783110336733.61.
[4] J. Kalms, A. Schmidt, S. Frielingsdorf, P. van der Linden, D. von Stetten, O. Lenz, P. Carpentier, P. Scheerer, Krypton derivatization of an O_2-tolerant membrane-bound [NiFe] hydrogenase reveals a hydrophobic tunnel network for gas transport, Angew. Chem. Int. Ed. Engl. 55 (18) (2016) 5586–5590, https://doi.org/10.1002/anie.201508976.
[5] M. Horch, L. Lauterbach, O. Lenz, P. Hildebrandt, I. Zebger, NAD(H)-coupled hydrogen cycling - structure-function relationships of bidirectional [NiFe] hydrogenases, FEBS Lett. 586 (5) (2012) 545–556, https://doi.org/10.1016/j.febslet.2011.10.010.
[6] M. Kuhn, A. Steinbüchel, H.G. Schlegel, Hydrogen evolution by strictly aerobic hydrogen bacteria under anaerobic conditions, J. Bacteriol. 159 (2) (1984) 633–639.
[7] S.J. Lin, L. Guarente, Nicotinamide adenine dinucleotide, a metabolic regulator of transcription, longevity and disease, Curr. Opin. Cell Biol. 15 (2) (2003) 241–246, https://doi.org/10.1016/S0955-0674(03)00006-1.
[8] M. Horch, P. Hildebrandt, I. Zebger, Concepts in bio-molecular spectroscopy: vibrational case studies on metalloenzymes, Phys. Chem. Chem. Phys. 17 (2015) 18222–18237, https://doi.org/10.1039/C5CP02447A.
[9] J.V. Rocheleau, W.S. Head, D.W. Piston, Quantitative NAD(P)H/flavoprotein autofluorescence imaging reveals metabolic mechanisms of pancreatic islet pyruvate response, J. Biol. Chem. 279 (30) (2004) 31780–31787, https://doi.org/10.1074/jbc.M314005200.
[10] G.H. Patterson, S.M. Knobel, P. Arkhammar, O. Thastrup, D.W. Piston, Separation of the glucose-stimulated cytoplasmic and mitochondrial NAD(P)H responses in pancreatic islet beta cells, Proc. Natl. Acad. Sci. U. S. A. 97 (10) (2000) 5203–5207, https://doi.org/10.1073/pnas.090098797.
[11] T.S. Blacker, Z.F. Mann, J.E. Gale, M. Ziegler, A.J. Bain, G. Szabadkai, M.R. Duchen, Separating NADH and NADPH fluorescence in live cells and tissues using FLIM, Nat. Commun. 5 (1) (2014) 3936, https://doi.org/10.1038/ncomms4936.
[12] D.S. Bilan, V.V. Belousov, Genetically encoded probes for NAD^+/NADH monitoring, Free Radic. Biol. Med. 100 (11) (2016) 32–42, https://doi.org/10.1016/j.freeradbiomed.2016.06.018.
[13] D. Williamson, P. Lund, H. Krebs, The redox state of free nicotinamide-adenine dinucleotide in the cytoplasm and mitochondria of rat liver, Biochem. J. 103 (2) (1967) 514–527, https://doi.org/10.1042/bj1030514.
[14] D.S. Bilan, M.E. Matlashov, A.Y. Gorokhovatsky, C. Schultz, G. Enikolopov, V.V. Belousov, Genetically encoded fluorescent indicator for imaging NAD^+/NADH ratio changes in different cellular compartments, Biochim. Biophys. Acta Gen. Subj. 1840 (3) (2014) 951–957, https://doi.org/10.1016/j.bbagen.2013.11.018.
[15] Y.P. Hung, J.G. Albeck, M. Tantama, G. Yellen, Imaging cytosolic NADH-NAD^+ redox state with a genetically encoded fluorescent biosensor, Cell Metab. 14 (4) (2011) 545–554, https://doi.org/10.1016/j.cmet.2011.08.012.
[16] Y. Zhao, J. Jin, Q. Hu, H.-M. Zhou, J. Yi, Z. Yu, X. Wang, Y. Yang, J. Loscalzo, Genetically encoded fluorescent sensors for intracellular NADH detection, Cell Metab. 14 (4) (2011) 555–566, https://doi.org/10.1016/j.cmet.2011.09.004.
[17] Y. Zhao, Y. Yang, Profiling metabolic states with genetically encoded fluorescent biosensors for NADH, Curr. Opin. Biotechnol. 31 (2015) 86–92, https://doi.org/10.1016/j.copbio.2014.08.007.
[18] G.S. Baird, D.A. Zacharias, R.Y. Tsien, Circular permutation and receptor insertion within green fluorescent proteins, Proc. Natl. Acad. Sci. U. S. A. 96 (20) (1999) 11241–11246, https://doi.org/10.1073/pnas.96.20.11241.
[19] E.A. Sickmier, D. Brekasis, S. Paranawithana, J.B. Bonanno, M.S.B. Paget, S.K. Burley, C.L. Kielkopf, X-ray structure of a Rex-family repressor/NADH complex insights into the mechanism of redox sensing, Structure 13 (1) (2005) 43–54, https://doi.org/10.1016/j.str.2004.10.012.
[20] E. Wang, M.C. Bauer, A. Rogstam, S. Linse, D.T. Logan, C. von Wachenfeldt, Structure and functional properties of the *Bacillus subtilis* transcriptional repressor Rex, Mol. Microbiol. 69 (2) (2008) 466–478, https://doi.org/10.1111/j.1365-2958.2008.06295.x.
[21] Y. Zhao, Q. Hu, F. Cheng, N. Su, A. Wang, Y. Zou, H. Hu, X. Chen, H.M. Zhou, X. Huang, K. Yang, Q. Zhu, X. Wang, J. Yi, L. Zhu, X. Qian, L. Chen, Y. Tang, J. Loscalzo, Y. Yang, SoNar, a highly responsive NAD^+/NADH sensor, allows high-throughput metabolic screening of anti-tumor agents, Cell Metab. 21 (5) (2015) 777–789, https://doi.org/10.1016/j.cmet.2015.04.009.
[22] B. Bennett, E. Kimball, M. Gao, Absolute metabolite concentrations and implied enzyme active site occupancy in *Escherichia coli*, Nat. Chem. Biol. 5 (8) (2009) 593–599, https://doi.org/10.1038/nchembio.186.
[23] Y. Zhao, Y. Yang, Frex and FrexH: indicators of metabolic states in living cells, Bioeng. Bugs 3 (3) (2012) 181–188, https://doi.org/10.4161/bbug.19769.
[24] Y. Zhou, L. Wang, F. Yang, X. Lin, S. Zhang, Z.K. Zhao, Determining the extremes of the cellular NAD(H) level by using an *Escherichia coli* NAD^+-auxotrophic mutant, Appl. Environ. Microbiol. 77 (17) (2011) 6133–6140, https://doi.org/10.1128/AEM.00630-11.
[25] V. Tejwani, F.-J. Schmitt, S. Wilkening, I. Zebger, M. Horch, O. Lenz, T. Friedrich, Investigation of the NADH/NAD^+ ratio in *Ralstonia eutropha* using the fluorescence reporter protein Peredox, Biochim. Biophys. Acta Bioenerg. 1858 (1) (2017) 86–94, https://doi.org/10.1016/j.bbabio.2016.11.001.
[26] S. Wilkening, F.-J. Schmitt, M. Horch, I. Zebger, O. Lenz, T. Friedrich, Characterization of Frex as an NADH sensor for *in vivo* applications in the presence of NAD^+ and at various pH values, Photosynth. Res. 133 (1–3) (2017) 305–315, https://doi.org/10.1007/s11120-017-0348-0.
[27] S. Gyan, Y. Shiohira, I. Sato, M. Takeuchi, T. Sato, Regulatory loop between redox sensing of the NADH/NAD^+ ratio by Rex (YdiH) and oxidation of NADH by NADH dehydrogenase Ndh in *Bacillus subtilis*, J. Bacteriol. 188 (20) (2006) 7062–7071, https://doi.org/10.1128/JB.00601-06.
[28] M. Horch, L. Lauterbach, M. Saggu, P. Hildebrandt, F. Lendzian, R. Bittl, O. Lenz, I. Zebger, Probing the active site of an O_2-tolerant NAD^+-reducing [NiFe]-hydrogenase from *Ralstonia eutropha* H16 by in situ EPR and FTIR spectroscopy, Angew. Chem. Int. Ed. 49 (2010) 8026–8029, https://doi.org/10.1002/anie.201002197.
[29] L. Kleihues, O. Lenz, M. Bernhard, T. Buhrke, B. Friedrich, The H_2 sensor of *Ralstonia eutropha* is a member of the subclass of regulatory [NiFe] hydrogenases, J. Bacteriol. 182 (10) (2000) 2716–2724, https://doi.org/10.1128/jb.182.10.2716-2724.2000.
[30] E.C. Hulme, M.A. Trevethick, Ligand binding assays at equilibrium: validation and interpretation, Br. J. Pharmacol. 161 (6) (2010) 1219–1237, https://doi.org/10.1111/j.1476-5381.2009.00604.x.

[31] S. Swillens, Interpretation of binding curves obtained with high receptor concentrations: practical aid for computer analysis, Mol. Pharmacol. 47 (6) (1995) 1197–1203.
[32] M. Schwarzländer, S. Wagner, Y.G. Ermakova, V.V. Belousov, R. Radi, J.S. Beckman, G.R. Buettner, N. Demaurex, M.R. Duchen, H.J. Forman, M.D. Fricker, D. Gems, A.P. Halestrap, B. Halliwell, U. Jakob, I.G. Johnston, N.S. Jones, D.C. Logan, B. Morgan, F.L. Müller, D.G. Nicholls, S.J. Remington, P.T. Schumacker, C.C. Winterbourn, L.J. Sweetlove, A.J. Meyer, T.P. Dick, M.P. Murphy, The 'mitoflash' probe cpYFP does not respond to superoxide, Nature 514 (7523) (2014) E12–E14, https://doi.org/10.1038/nature13858.
[33] R. Sander, Compilation of Henry's law constants (version 4.0) for water as solvent, Atmos. Chem. Phys. 15 (2015) 4399–4981, https://doi.org/10.5194/acp-15-4399-2015.
[34] Engineering ToolBox (2008). Diffusion coefficients of gases in water. [online] available at: https://www.engineeringtoolbox.com/diffusion-coefficients-d_1404.html [accessed July 17,2019].
[35] R.N. Day, M.W. Davidson, The fluorescent protein palette: tools for cellular imaging, Chem. Soc. Rev. 38 (10) (2009) 2887–2921, https://doi.org/10.1039/b901966a.
[36] K. Schneider, H.G. Schlegel, Purification and properties of soluble hydrogenase from *Alcaligenes eutrophus* H 16, Biochim. Biophys. Acta, Enzymol. 452 (1) (1976) 66–80, https://doi.org/10.1016/0005-2744(76)90058-9.
[37] J.T. Larsson, A. Rogstam, C. von Wachenfeldt, Coordinated patterns of cytochrome bd and lactate dehydrogenase expression in *Bacillus subtilis*, Microbiology 151 (10) (2005) 3323–3335, https://doi.org/10.1099/mic.0.28124-0.
[38] K.J. McLaughlin, C.M. Strain-Damerell, K. Xie, D. Brekasis, A.S. Soares, M.S.B. Paget, C.L. Kielkopf, Structural basis for NADH/NAD^+ redox sensing by a Rex family repressor, Mol. Cell 38 (4) (2010) 563–575, https://doi.org/10.1016/j.molcel.2010.05.006.